DETECTION OF FLOW SEPARATION USING MICROPHONE ARRAYS

Raimund Perschke, Rakesh C. Ramachandran and Ganesh Raman
Fluid Dynamic Research Center, Illinois Institute of Technology
10 W 32nd street, 60616, Chicago, IL, USA.
(Raman@iit.edu)

ABSTRACT

The role of microphone phased arrays as a tool to detect flow separation is investigated. A backward-facing step is used to create a separated flow, thereby inducing a region of elevated free-stream turbulence downstream of the step. Velocity measurements and a flow visualization technique are used to complement microphone measurements. It is shown that flow separation can be distinguished from flow-edge interaction noise due to their different dependencies on Mach number and observation angle. Flow separation noise is produced several centimeters downstream of the flow-edge interaction noise and is more dominant at high Mach numbers. The performance of the beamforming algorithms TIDY, DAMAS2, and CLEAN-SC are evaluated. It is observed that all the beamforming algorithms provide good separation of free-stream noise and flow-edge interaction noise at the relatively high frequencies considered although CLEAN-SC tends to yield output powers that are typically 3 dB lower.

1 INTRODUCTION

Microphone phased arrays have become a widely used tool for noise measurements. One of their advantages is that most dominant acoustic sources at reasonable distance to the array can be detected and localized with a single measurement. As such, beamforming has found use in many engineering applications where the main interest is to determine the principal causes of noise production or to assess mitigation strategies. An extensive overview of the different areas of application is given in [5].

In this paper, the detection and localization of flow separation via a microphone phased array is described. In this regard beamforming represents a new application of non-intrusive measurement technique. The objective of detecting and localizing separated flows acoustically is possible because separated flows often exhibit higher levels of turbulence than attached flows

which leads to higher acoustic pressures being generated. One major difficulty with this approach is to discriminate between different sources of flow-induced sound. Turbulent flow over the edge of a backward-facing step is known to produce trailing edge scattering noise which can dominate any other mechanisms of sound production. In the remainder of this paper the authors describe their approache to isolating free-stream sound from other sound sources in the vicinity of the step using a compact and mobile 24-channel microphone phased array.

2 EXPERIMENTAL DATA ANALYSIS

2.1 The beamforming array

A commercially available 24-channel OptiNav Array 24 microphone phased array was used for source localization. The microphones are based on the Panasonic WM-61A electret capsule. The array uses a non-redundant sensor layout in a compact octagonal mounting board of 91 cm diagonal. A digital camera of 640×480 pixels resolution in the center of the array can be used to overlay beamform maps with pictures or videos taken of the area under investigation. Data acquisition is provided by a MOTU 24I/O 24-channel chassis. Each channel has 24-bit resolution and interfacing to a laptop computer with the recording software is established via a PCIe-424 MAGMA Express Box.

The 3-dB beamwidth of the array was evaluated for conventional beamforming. The result for a single speaker placed 50 cm in front of the array is shown in Fig. 1(a). The solid lines represent the point spread function of a simulated source at the respective location. The steering vector contains values derived from the free-space Green's function and diagonal deletion is applied to the simulated cross-spectral matrix as outlined in [1].

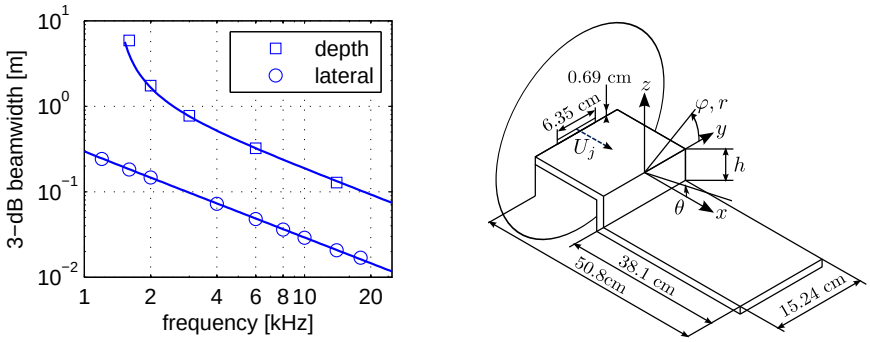

Figure 1: (a) Array resolution for a point source 50 cm in front of its center. Markers represent measured values and solid lines are obtained from simulated point spread functions. (b) Geometry of the setup and coordinate system with the flow direction

Beamforming is performed in a plane parallel to the array. The spacing of the internal beamforming grid is a fraction of the Rayleigh resolution ([4]) and is given as

$$\Delta x = \frac{R}{6r} \tag{1}$$

where R is the Rayleigh resolution for the array and r is a user parameter that is chosen as

$r = 0.75$. TIDY [3], DAMAS2 [2], and CLEAN-SC [6] beamforming algorithms are used to create beamform maps which are are overlayed with graphical representations of the setup to facilitate the identification of noise sources.

2.2 Experimental setup

The experimental data was acquired at the IIT anechoic high-speed jet facility. The setup is shown in Fig. 1(b). Air is supplied at room temperature to the anechoic chamber ($2.2 \times 2 \times 4$ m^3) and exits through a rectangular outlet. The rectangular jet opening has dimensions of 6.35 cm width and 0.69 cm height and is placed in the center of a circular inlet of 30.48 cm diameter. The backward-facing step has a width of 15.24 cm and a total length of 38.1 cm. The upper part has a length of 12.7 cm and the step height is adjustable from 0 cm to 5.08 cm in increments of 1.27 cm. The lower plate is terminated by a serrated trailing edge to reduce scattering of hydrodynamic pressure fluctuations. The test object allows for side walls to be mounted onto the plates, creating a channel of 5.08 cm height between $y = \pm 3.81$ cm. During the experiments, the inlet was covered with acoustic foam to minimize acoustic reflections and scattering from the rim. The array was left uncovered but pressure doubling at the microphones was accounted for by subtracting 6.02 dB from the beamformer output power and measured sound pressure levels.

Two scenarios are considered in this paper: in the first case, no side walls are attached to the step and in the second case, the side walls are attached to create a channel. For this purpose, the array is placed at $(x,r) = (10\text{ cm}, 50\text{ cm})$ at angles of $\varphi = 15^\circ, 45^\circ, 90^\circ$ facing towards the jet centerline. In the case of the channel flow the observation angle is restricted to $\varphi = 90^\circ$.

The sampling frequency in the measurements was 44,100 Hz with internal anti-aliasing filters appropriately set. The data acquisition time was 25 s. Optinav Beamform Interactive software was used to compute cross-power spectral densities according to Welch's method of averaged cross-periodograms, using a transform length of 2048, a Hanning window weighting of the data blocks, and 50% overlap which resulted in a narrow-band bandwidth of 21.5 Hz and a total number of 1075 data blocks per channel.

2.3 Flow visualization and velocity measurements

A mixture of an alkyd resin based painting medium, oil paint, and vegetable oil was used for flow visualization. 2 μL of the mixture were distributed on each node of a rectangular grid of 5 mm spacing. For the channel flow, the unguided flow, and the upper plate, an oil-alkyd mixture ratio of 1 : 1, 4 : 1, 1 : 0 was used, respectively. This yielded a viscosity that rendered the applied pattern independent of transient start-up processes. Figure 2 shows the applied pattern before and after the jet was started for the case $h = 5.04$ cm, Ma $= 0.6$, and the side walls mounted during the run (removed in the pictures). The trajectories are shown in Fig. 2 and composite images in isometric projection are shown in Fig.3 and Fig.10.

Figure 10 displays that significant backflow is attained in the recirculation region. The re-circulating fluid shows a three dimensional behavior in the case of $h <= 3.81$ cm. The flow visualization technique in Fig. 3 reveals no features of a recirculating fluid in the free step flow.

For the channel flow, two locations on the lower plate become visible that display radially diverging trajectories. Furthermore, there appears one position where the trajectories point into opposite streamwise directions.

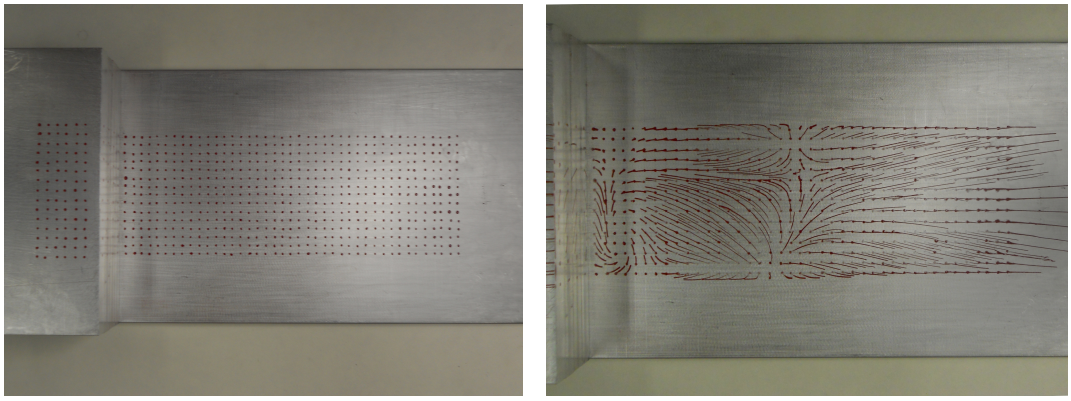

Figure 2: Result of the flow visualization technique for the channel flow at $h = 5.08$ cm and $\mathrm{Ma} = 0.6$

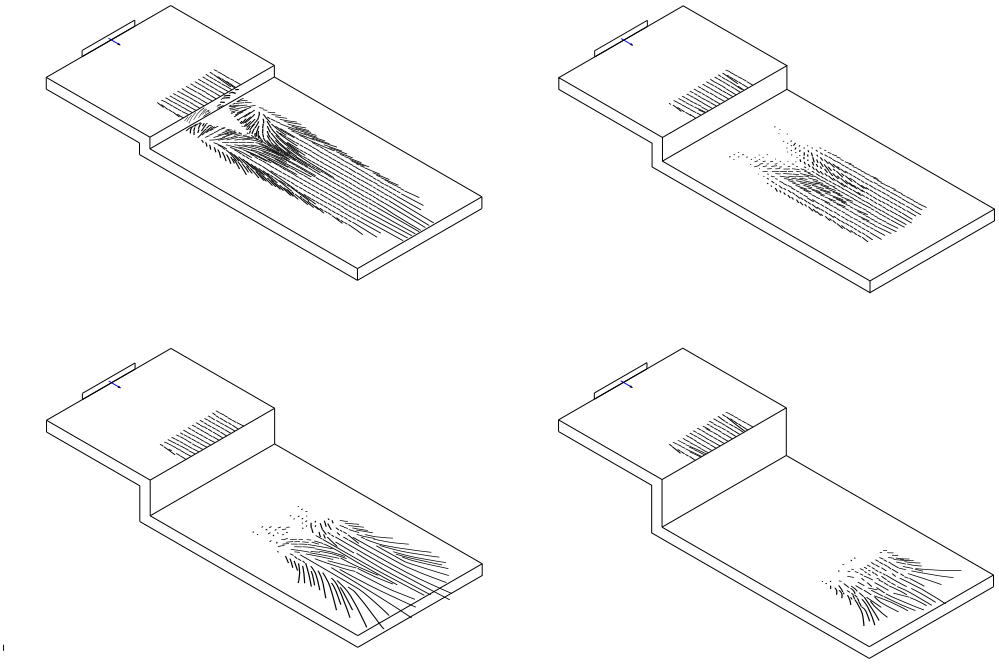

Figure 3: Trajectories of the oil paint flow visualization for $\mathrm{Ma} = 0.6$ *without side walls*

Measurements of the velocity profile at $y = 0$ cm were taken with a Pitot probe of 0.5 mm diameter at a representative Mach number of $\mathrm{Ma}_{ref} = 0.3$. Figure 4 shows a comparison of the x-component of the velocity for different step heights and streamwise positions. There is generally no backflow for the case without side walls. For the channel flow, the velocity attains a magnitude of $0.45 \cdot \mathrm{Ma}_{ref}$ in the recirculation region.

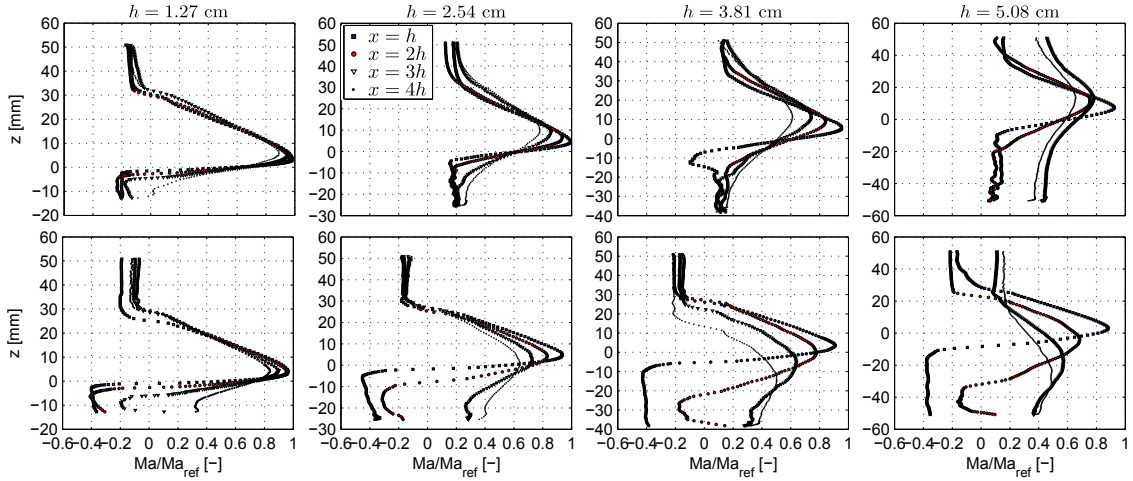

Figure 4: Velocity profile for $\mathrm{Ma}_{ref} = 0.3$ *obtained by measurements with a Pitot probe*

2.4 Shear layer correction

To assess the effect of the flow on the ability to accurately localize sources within the flow a Pyramid TW44 tweeter was flush mounted underneath a perforated backward-facing step of identical dimensions to the one described in Sec. 2.2. To suppress resonance and to mitigate broadband sound generated by the interaction of the flow with the holes the surface of the object was covered with a polyester cloth. The tweeter was fed with bandpass filtered Gaussian white noise. The displacement of the location of highest output power determined by delay-and-sum beamforming over a frequency range of $f = 6$ kHz…19 kHz was measured. Shown in the first row of Fig. 5 is the displacement versus inflow Mach number for various streamwise locations of the tweeter for the flat plate. The second row shows values of the displacement at the streamwise position of reattachment as obtained from the flow visualization technique and at $x = 5$ cm for different step heights. Note that the tweeter was at least 20 dB, 15 dB, and 10 dB louder than any flow generated source at Mach numbers of $\mathrm{Ma} = 0.1 \ldots 0.25$, $\mathrm{Ma} = 0.3 \ldots 0.5$, and $\mathrm{Ma} = 0.55 \ldots 0.6$ respectively as sensed by the array.

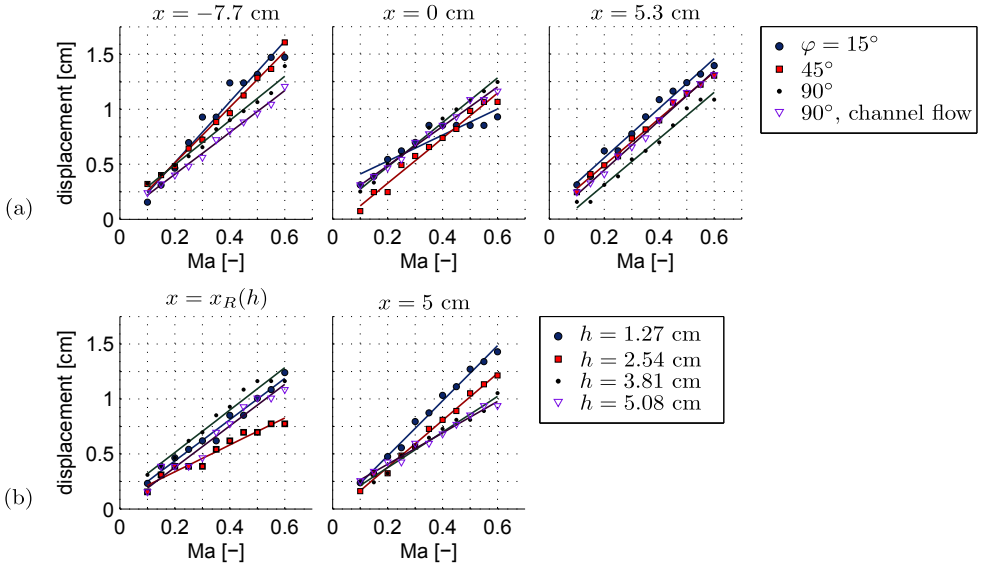

Figure 5: Streamwise displacement of the array peak output power as a function of inflow Mach number and position of the source

2.5 Far-field microphone measurements

The sound pressure levels over a frequency range of 1 kHz to 22 kHz for the channel flow and the free step flow were measured using a Brüel & Kjær Type 4939 condenser microphone at nine locations in the x-z-plane on a semicircle of radius 0.6 m around the origin of the coordinate system, as shown in Fig. 6. The values for the angle θ were obtained by interpolating the array sound pressures and using an amplitude correction to scale it to a distance of 0.6 m.

A comparison between the channel flow and the free flow shows that the presence of the side barriers increases the sound pressure level most significantly under shallow angles of $\theta < 45°$. With higher Mach number the radiated sound pressure becomes less directional. The increase in sound pressure level due to addition of the side barriers is greatest at $\mathrm{Ma} = 0.6$ and $\varphi = 20°$.

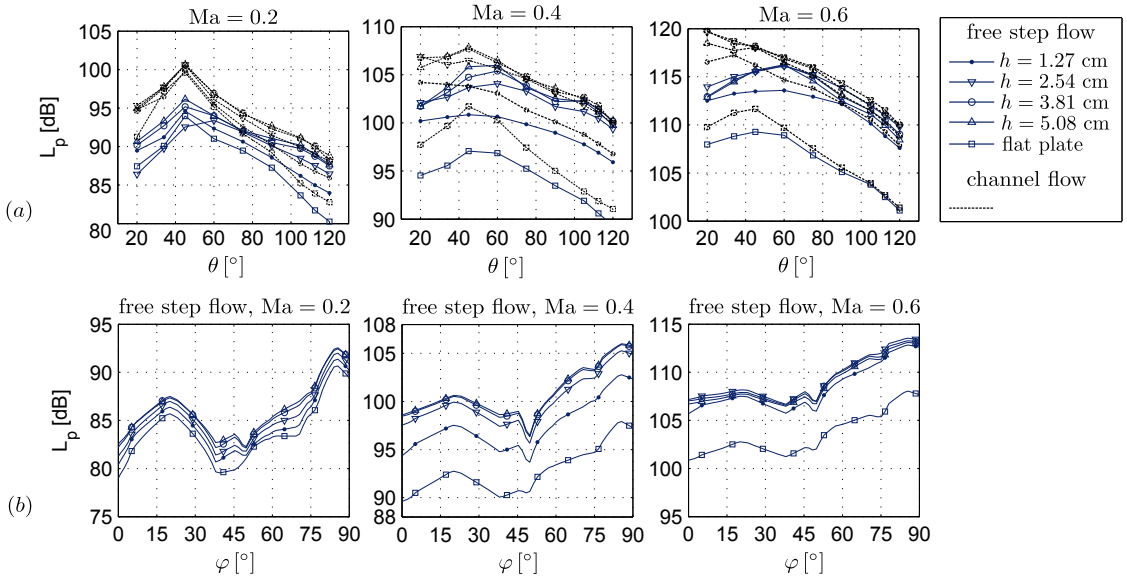

Figure 6: Far-field directivity for the channel flow and free step flow

2.6 Source localization

A comparison of the algorithms TIDY, DAMAS2, and CLEAN-SC is presented in Fig. 7. The results demonstrate that the algorithms detect flow-edge interaction noise as well as free-stream turbulence noise. The peak output levels and locations of the maxima show good agreement between TIDY and DAMAS2 whereas CLEAN-SC offers values that are typically by about 3 dB lower. The algorithms reveal the same main features where DAMAS2 gives the clearest acoustic representations and CLEAN-SC tends to suppress non-dominant output power. In the top view, the algorithms locate the maxima of the flow-edge interaction noise at $x = 1.4$ cm and the free-stream noise at $x = 4.4$ cm.

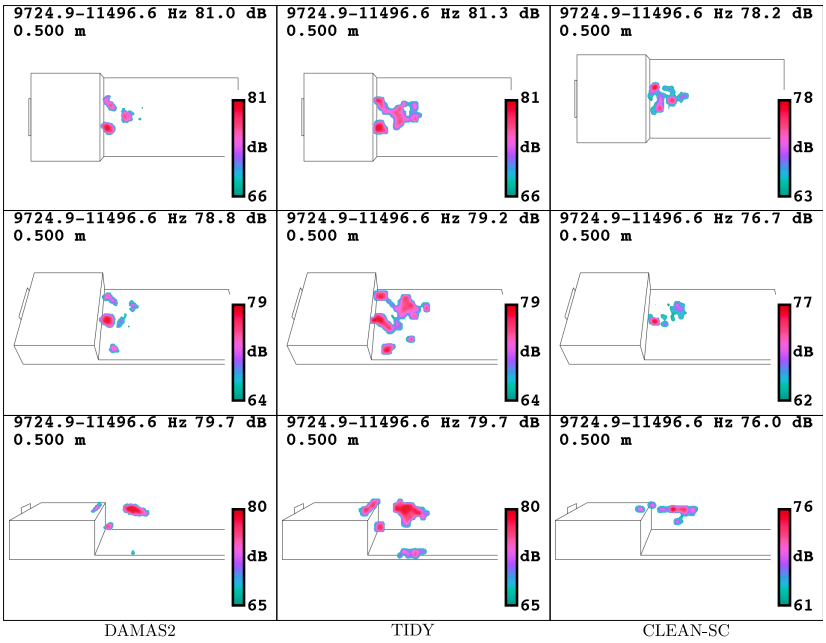

Figure 7: Comparion of TIDY, DAMAS2, and CLEAN-SC beamforming algorithms for Ma $=$ 0.6 *and* $h = 5.08$ *cm*

A source integration technique is employed to find the dependency of the different noise sources on Mach number and observation angle in the free step flow. Two regions are defined: the first one encompasses the region downstream of the step (2 cm $\leq x \leq$ 10 cm) and is intended to capture the free-stream noise. The second one encompasses the step (-2 cm $\leq x \leq$ 2 cm). To allow for true separation of the different sources the lower frequency limit is determined by the Rayleigh criterion for sufficient resolution ($f = 6800$ Hz). The upper frequency limit is given by the Nyquist frequency. The results are given in Fig. 8. They show that free-stream noise follows a power law to a higher power than acoustic sources from the edge region when observed from $\varphi = 15°$. As the observation angle increases the results suggest a lower power law behavior such that the Mach number dependency approaches the behavior of the sources from the step region.

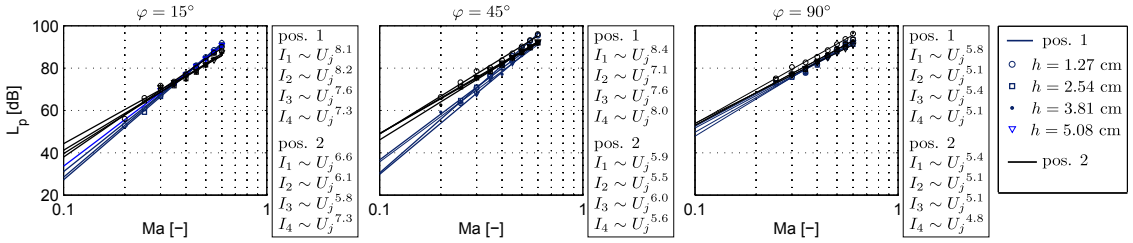

Figure 8: Mach dependency

The channel flow is examined in Fig. 9. The first, second, and third row show beamform maps for varying step heights obtained with TIDY, CLEAN-SC, and DAMAS2, respectively. Row four offers TIDY results for the free step flow for comparison. The beamform maps for

the channel flow show stronger turbulence noise than the ones for the free step flow. Distinct maxima become apparent in the vicinity of the side barriers that are mostly detected by TIDY. Their streamwise origin is correlated with the locations of radially diverging trajectories as can be seen in Fig. 10. A slight asymmetry in the beamform maps with respect to the jet centerline is noticeable for $h \geq 2.54$ cm. DAMAS2 shows the same main features but only indicates a peak near the side barrier for $h = 2.54$ cm. CLEAN-SC shows none of the features in the vicinity of the wall and shows little variation in cross-stream position of the main source. The free step flow shows no significant change in streamwise extent of the turbulence region with varying step height. This is in contrast to the channel flow where TIDY shows a longer region of significant output power with increasing step height.

Figure 10 combines results from the flow visualization experiment with beamforming results for Ma $= 0.6$. A shear layer correction for the flat plate case with the source at $x = 0$ cm has been applied (refer to Fig. **??**). It can be observed that the three-dimensional behavior of the flow in the recirculation region is correlated with the location and size of the array output power.

To assess the influence of the side walls on the beamform map a Pyramid TW44 tweeter was placed at various streamwise positions underneath the lower plate of the step with the side walls attached and removed. The tweeter was again fed with Gaussian white noise and no distinct maxima are observed near the side walls. An example for the tweeter at $x = 2$ cm and $h = 1.27$ cm without using the region-of-interest technique to exclude sidelobes is given in Fig. 9(b). Figure 9(c) shows the beamforming result with the lower plate removed. In this setup, the free-stream turbulence noise generates a lower output power and appears symmetrical about the jet centerline in the beamform map.

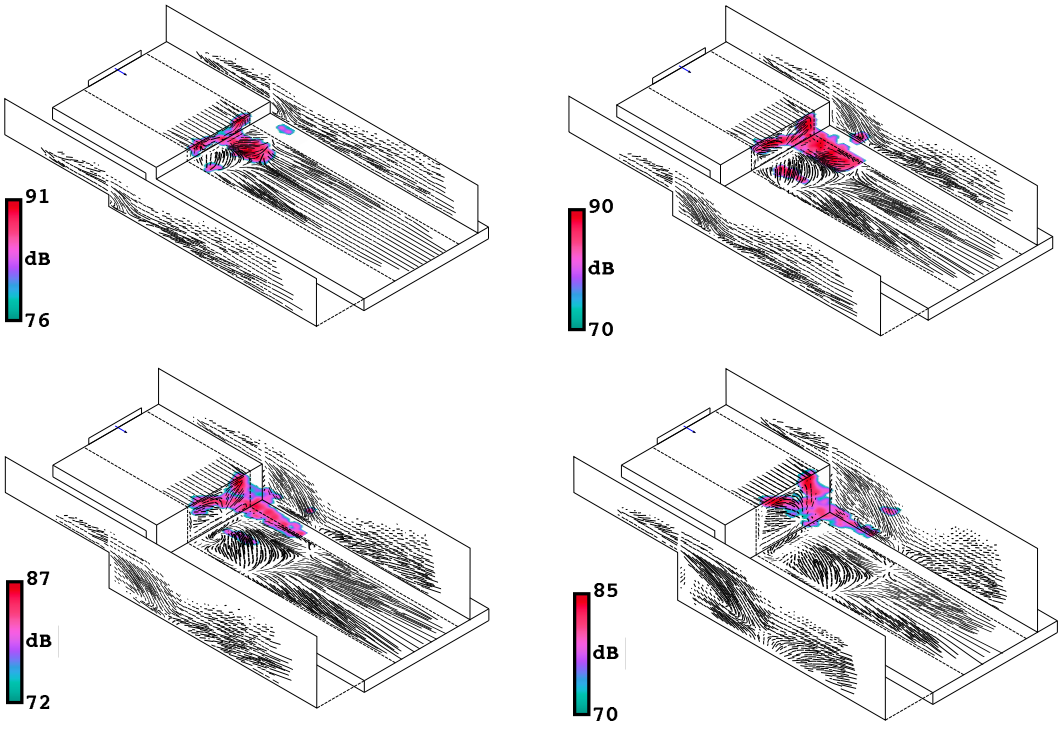

Figure 10: Results of beamforming for $f = 8kHz \ldots 16kHz$ and $Ma = 0.6$ using TIDY combined with results from the flow visualization experiment in isometric projection

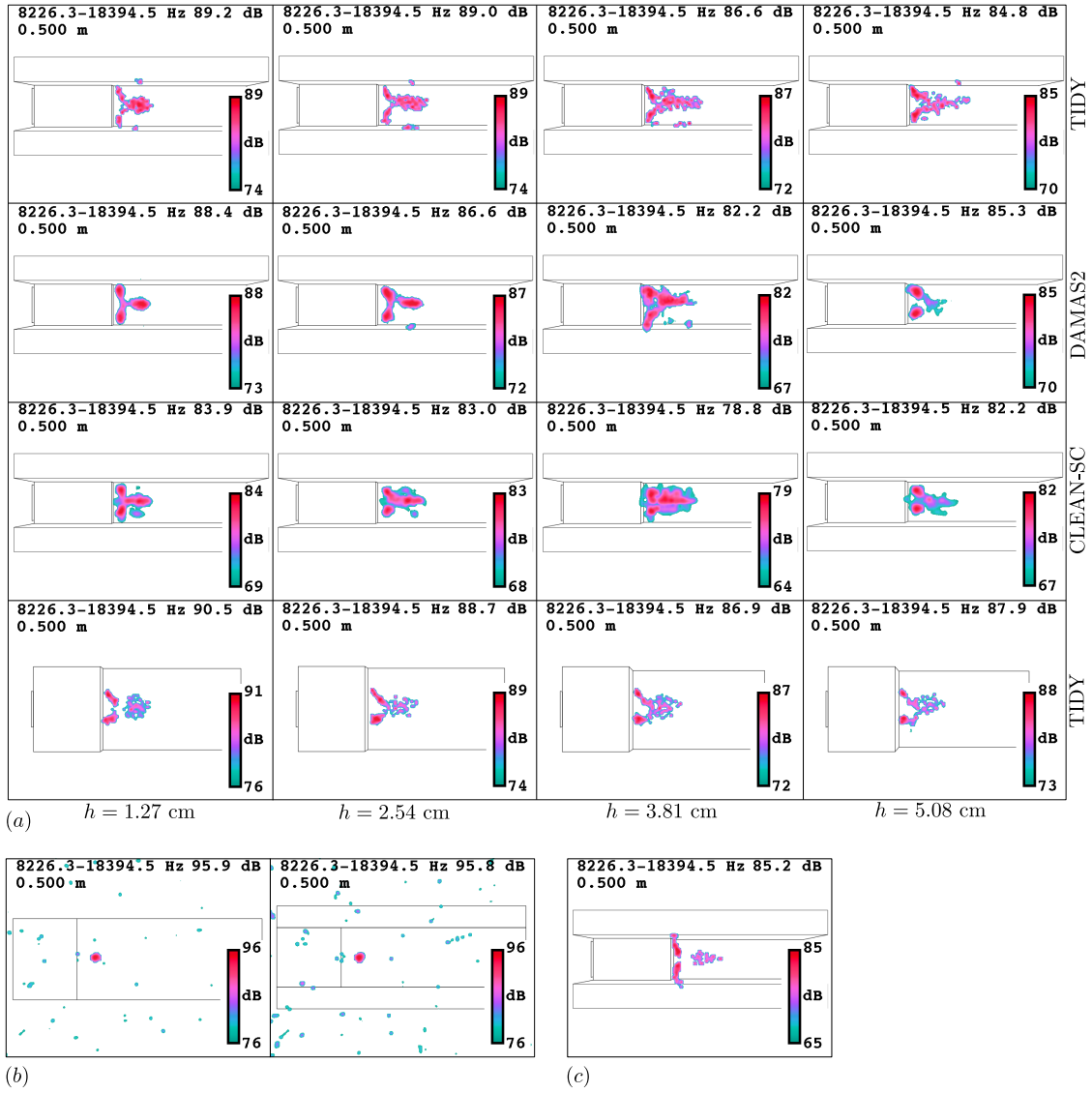

Figure 9: (a) Result of beamforming for a frequency range of $f = 8kHz \ldots 18kHz$ and $\mathrm{Ma} = 0.6$. (b) Point spread function for a tweeter placed in the center of the channel at $x = 2$ cm and $h = 1.27$ cm. (c) Result of beamforming with TIDY with the lower plate of the step removed

3 CONCLUSIONS

The noise production of a flow over a backward-facing step has been examined. The wall-jet separates at the edge and produces free-stream sound that can be detected with microphones. Additional sources exist in the vicinity of the edge due to the interaction of the turbulent boundary layer with the structure. These two mechanisms of sound production can be discriminated using microphone arrays when the analysis frequencies are sufficiently high because the maximum of the free-stream sound is produced some distance downstream of the edge. It is found

that the array placed sideways to the step detects acoustic power that has an average dependency of $Ma^{7.8}$ for the sound from the source region as opposed to an average $Ma^{6.5}$ dependency for sound from the region around the step. With larger observation angles φ the Mach number dependencies approach each other and thus become less favorable for detection of flow separation.

Of the examined beamforming algorithms TIDY, CLEAN-SC, and DAMAS2 all were able to detect free-stream sound. A good agreement of absolute output levels between TIDY and DAMAS2 was observed whereas CLEAN-SC tended to give values that were lower by 3 dB. Higher acoustic power is detected by the beamforming algorithms in the region downstream of the edge in the case of the channel flow compared to the free flow. This is in accordance with measurements of the velocity profile that suggests up to 45% higher shear velocities. Contrary to the unguided flow, the channel flow shows an asymmetry of array output power in the recirculation region with respect to the jet centerline except for the lowest step height. The flow visualization technique reveals such an asymmetry in the afore mentioned cases.

4 ACKNOWLEDGEMENT

The experimental research reported in this work was funded by Jacobs/Air Force Research Lab (AFRL), Wright Patterson AFB, OH. The encouragement of Dr. Michael Stanek (AFRL) and Dr. Rudy Johnson (AFRL) is gratefully acknowledged.

REFERENCES

[1] R. P. Dougherty. “Beamforming in acoustic testing.” In *Aeroacoustic measurements* (edited by T. J. Mueller). Springer, Berlin, 2002.

[2] R. P. Dougherty. “Extensions of damas and benefits and limitations of deconvolution in beamforming, aiaa 2005-2961.” *11th AIAA/CEAS Aeroacoustics Conference (26th AIAA Aeroacoustics Conference), Monterey, California*, 2005.

[3] R. P. Dougherty. “Jet noise beamforming with several techniques: Bebec-2010-17.” *Berlin Beamforming Conference*, 2010.

[4] D. H. Johnson and D. E. Dudgeon. *Array signal processing: Concepts and techniques*. P T R Prentice Hall, Englewood Cliffs and NJ, 1993.

[5] U. Michel. “History of acoustic beamforming.” 2006.

[6] P. Sijtsma. “Clean based on spatial source coherence.” *International Journal of Aeroacoustics*, 6(4), 357–374, 2007.